Equivalent Hazard Magnitude Scale

Yi Wang (y.v.wang@unc.edu)
University of North Carolina at Chapel Hill https://orcid.org/0000-0003-2228-7009

Antonia Sebastian
University of North Carolina at Chapel Hill

Article

Keywords: Natural Hazard Management, Cross-hazard Evaluations, Regression-based Methodology, Tsunami, Drought, Tornadoes, Resource Allocation

Posted Date: December 28th, 2020

DOI: https://doi.org/10.21203/rs.3.rs-117402/v1

Equivalent Hazard Magnitude Scale

Yi (Victor) Wang[1*] & Antonia Sebastian[2]

[1]Department of Geological Sciences, University of North Carolina at Chapel Hill, Chapel Hill, NC, USA. e-mail: y.v.wang@unc.edu

[2]Department of Geological Sciences, University of North Carolina at Chapel Hill, Chapel Hill, NC, USA. email: a.sebastian@unc.edu

Abstract

Effective management of natural hazards requires the capability of cross-hazard evaluations. However, existing hazard magnitude scales cannot be easily adapted to evaluate sizes of events across different hazard types. Here, we propose a regression-based methodology with historical data on hazard impacts and magnitude indicators worldwide from 1900 to 2020 to derive an equivalent magnitude scale, called the Gardoni Scale after Professor Paolo Gardoni, to effectively quantify and compare sizes of events across twelve natural hazard types. Our results suggest that when compared on the Gardoni Scale, tsunami and drought disasters tend to have large magnitudes, while tornadoes are relatively small in size. We further propose hazard equivalency as a new area of research for cross-hazard evaluations of sizes and intensities of natural hazard events. Continuing efforts in this new area will strengthen guidance for resource allocation for hazard management, facilitate disaster communication, and enhance risk analysis within a multi-hazard context.

Introduction

Hazard scales for natural hazards indicate potential severity of natural hazard events. In general, there are two groups of hazard scales. We call the first group *agential scales*. An agential scale describes the size of the agent of a hazard event. Examples of agential scales include the earthquake Richter magnitude[1], the hurricane Saffir-Simpson wind scale[2], and the tornado enhanced Fujita scale[3,4]. The second group is called *locational scales*. A locational scale indicates the intensity of a hazard event experienced by entities at specific locations. Examples of locational scales include the earthquake modified Mercalli intensity scale[5,6], the integrated tsunami intensity scale[7], and the heat index for heatwaves[8,9]. Regarding agential scales, we classify some of them as unique-value scales, where there is only one unique value of a unique-value scale for one individual hazard event. As an example, the earthquake Richter magnitude[1] is a unique-value scale. We call the other agential scales temporally variant scales, where there can be multiple values of a temporally variant scale corresponding to one single hazard event during the entire process of the event. An example of temporally variant scale is the Saffir-Simpson hurricane wind scale[2]. For a temporally variant scale, however, we may still derive a unique value by, for example, selecting the maximum value of the scale. In this study, we use the term *magnitude scale* to refer to a unique-value agential hazard scale indicating the size of a natural hazard event.

Magnitude scales are widely adopted in professional practices in disaster and emergency management[10,11] regarding individual natural hazards such as earthquake[1,12,13], tsunami[14,15], landslide[16,17], volcanic activity[18,19], tropical cyclone[20–22] and drought[23,24]. However, these scales cannot be used to compare sizes of events across different natural hazard types. To enable evaluation of sizes of events across natural hazards, we propose an *equivalent magnitude scale* - the *Gardoni Scale* - for natural hazards. The proposed scale is named after the Alfredo H. Ang

Family Professor Paolo Gardoni[25,26] from the University of Illinois at Urbana–Champaign. Because, for each hazard type, the size of a natural hazard event is correlated with the expected adverse impact of the event, the expectation of impact can be used to provide information on the equivalency of event size with respect to events of different hazard types. Correspondingly, we designed the proposed equivalent magnitude as the expectation value of an *impact metric* of the event, where the impact metric is a function of impact variables. Using data on adverse impacts of natural disaster events from the EM-DAT International Disaster Database[27], we selected fatality, total affected population, and total damage in 2019 US dollars (USD) as three impact variables to construct the impact metric. The standardized natural logarithms of the selected three impact variables are positively correlated with each other (see Figs. 1a-1i and Supplementary Information Video 1). The principal component[28,29] of the standardized and logarithmically transformed impact variables was derived as the impact metric (see Figs. 1j-1m and Supplementary Information Video 1).

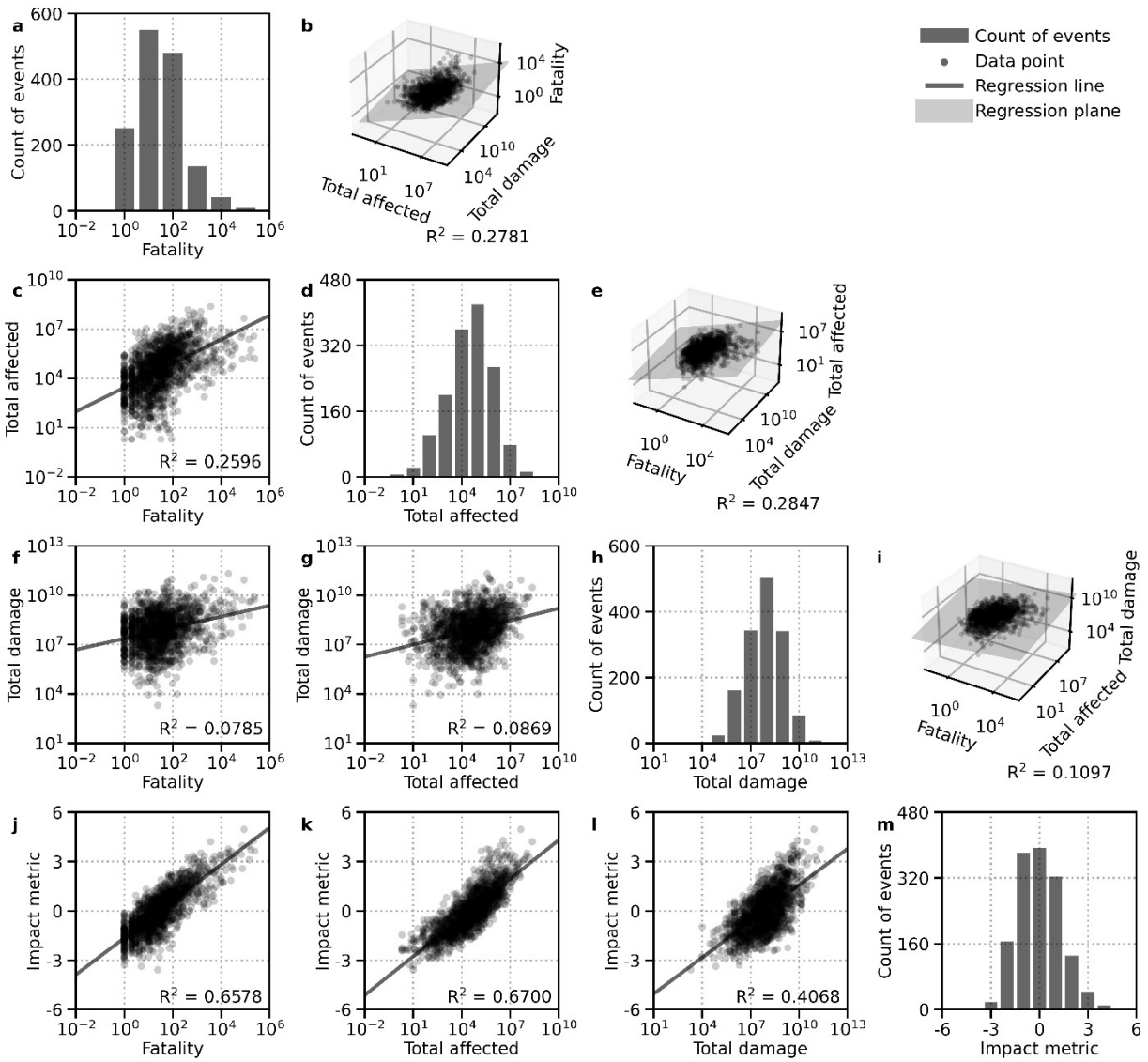

Fig. 1: Impact variables and impact metric. a, Histogram of impact variable fatality. **b**, Fatality regressed on total affected population and total damage in 2019 USD with a multiple linear regression. **c**, Total affected population regressed on fatality with a simple linear regression. **d**, Histogram of impact variable total affected population. **e**, Total affected population regressed on fatality and total damage in 2019 USD with a multiple linear regression. **f**, Total damage in 2019 USD regressed on fatality with a simple linear regression. **g**, Total damage in 2019 USD regressed on total affected population with a simple linear regression. **h**, Histogram of impact variable total

damage in 2019 USD. **i**, Total damage in 2019 USD regressed on fatality and total affected population with a multiple linear regression. **j**, Impact metric regressed on fatality with a simple linear regression. **k**, Impact metric regressed on total affected population with a simple linear regression. **l**, Impact metric regressed on total damage in 2019 USD with a simple linear regression. **m**, Histogram of impact metric.

To demonstrate the methodology for computing the equivalent magnitudes on the Gardoni Scale, we consider twelve natural hazards (see Fig. 2). For each hazard, we conducted a simple linear regression to derive the relationship between a magnitude indicator of the hazard as the independent variable and the impact metric as the dependent variable (see Fig. 2). The derived expected impact metric was then applied with a same linear transformation to fit within a range of roughly [0, 10] for all considered natural hazard events. The linearly transformed expectation of impact metric, shown with the expectation line in Fig. 3, is the equivalent magnitude proposed in this study. Although the equivalent magnitudes of natural hazard events are shown within a limited range (Fig. 3), the actual range of their possible values is $(-\infty, \infty)$.

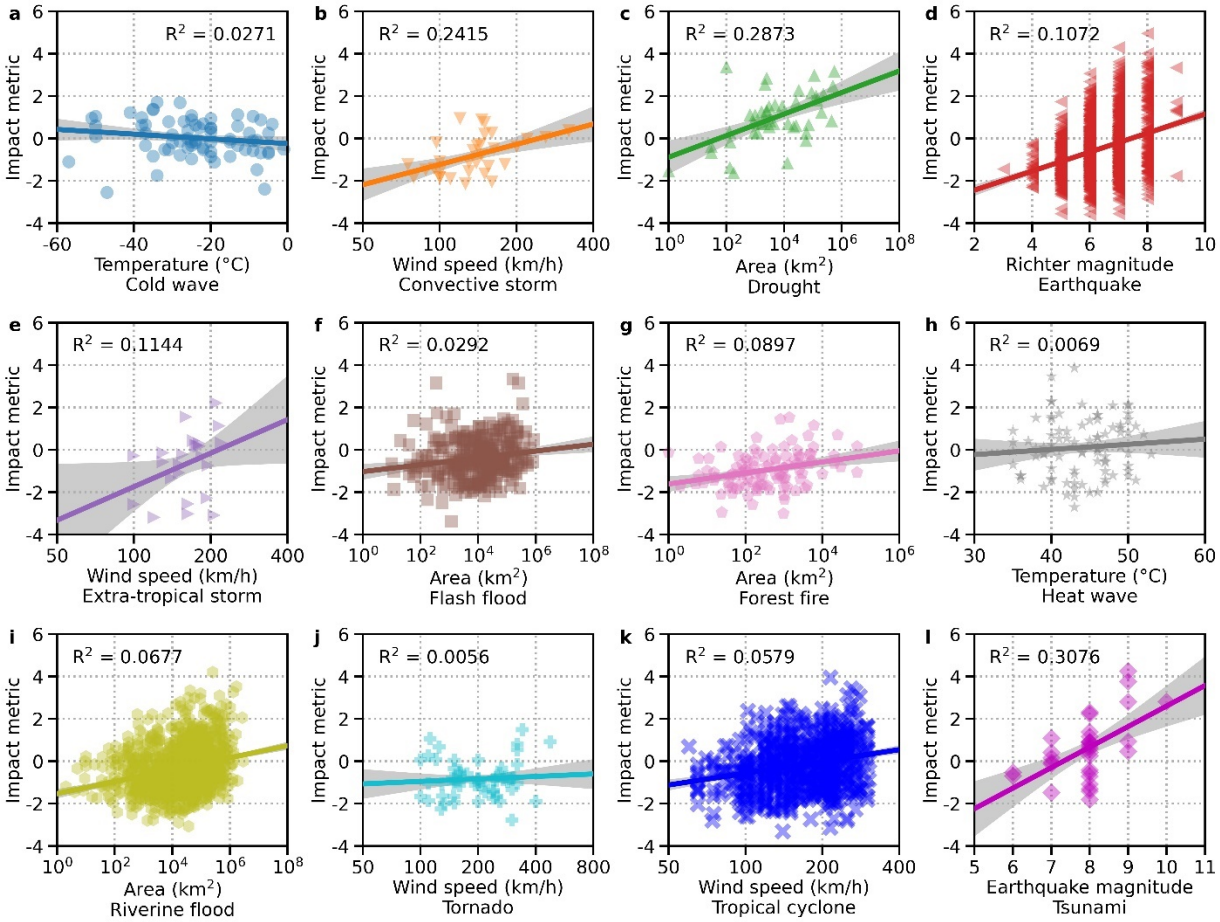

Fig. 2: Simple linear regressions on impact metric against magnitude indicators. a, Impact metric regressed on minimum temperature of cold wave. **b**, Impact metric regressed on peak gust wind speed of convective storm. **c**, Impact metric regressed on total area of drought. **d**, Impact metric regressed on Richter magnitude of earthquake. **e**, Impact metric regressed on peak gust wind speed of extra-tropical storm. **f**, Impact metric regressed on total flooded area of flash flood. **g**, Impact metric regressed on total burnt area of forest fire. **h**, Impact metric regressed on maximum temperature of heat wave. **i**, Impact metric regressed on total flooded area of riverine flood. **j**, Impact metric regressed on peak gust wind speed of tornado. **k**, Impact metric regressed on maximum sustained wind speed of tropical cyclone. **l**, Impact metric regressed on earthquake

magnitude of tsunami. Solid lines are regression lines. Shaded areas are the 95% confidence intervals of the corresponding regression lines.

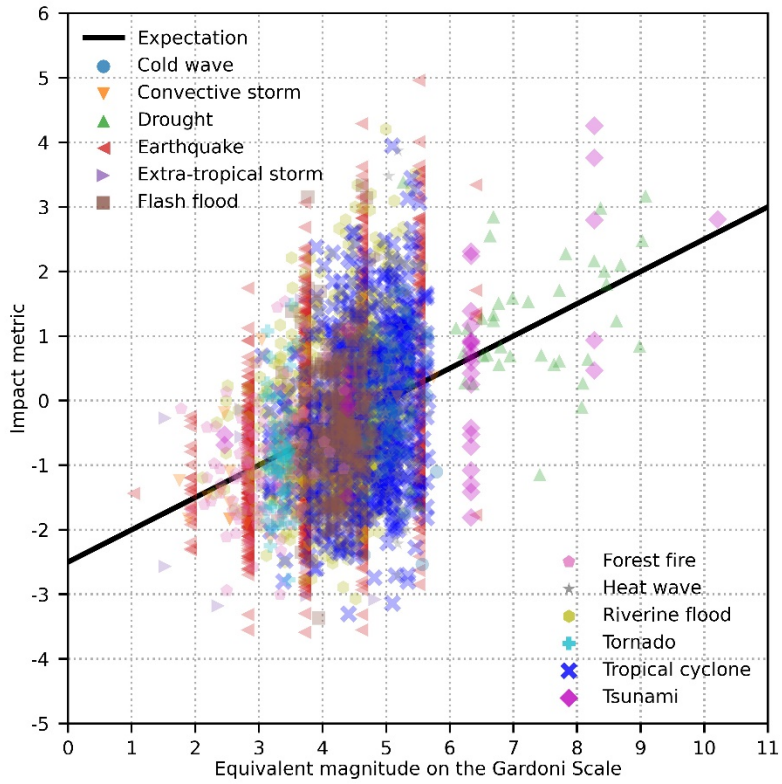

Fig. 3: Impact metric versus equivalent magnitude. The expectation line shows the values of the expected impact metric with respect to equivalent magnitude on the Gardoni Scale.

Results

Comparisons of hazard magnitudes

Because only those natural hazard events resulting in significant adverse impacts are included in the EM-DAT database[27], we expect that numerous events with small sizes had been left out before the data was collected and processed in this study. The data points presented in Fig. 3, therefore, only correspond to the tail part of the entire distribution of hazard events for each natural hazard. To compare different natural hazards regarding the sizes of their events, we focus on the events with large equivalent magnitudes. All 37 events with the largest equivalent magnitudes are either a tsunami or a drought, with their equivalent magnitudes ranging [6.50, 10.21]. The hazard event with the largest equivalent magnitude is the 1960 Chilean tsunami that killed 6,000 and affected over 2 million population in Chile as well as resulted in 61 fatalities in Hawaii, USA. The well-known 2004 Indian Ocean tsunami that killed more than 2 million people ranks 10th among all events, with its equivalent magnitude at 8.27. The drought event with the largest equivalent magnitude (9.07) is the 2002 Indian monsoon drought that affected a total of about 300 million people. The largest earthquake events, with equivalent magnitude at 6.41, include the 1920 Haiyuan earthquake in China that resulted in at least 180,000 fatalities. Among the considered twelve hazard types, the natural hazard with the lowest maximum equivalent magnitude is tornado. The tornado event with the largest equivalent magnitude (3.62) is the 2013 El Reno tornado in Oklahoma, USA, which led to a total damage of about 3.4 billion 2019 USD.

With the derived equivalent magnitudes on the Gardoni Scale, we are able to compare events of different natural hazard types, such as earthquake, tornado, forest fire, and tropical cyclone (see Fig. 4). According to the derived equivalent magnitudes of hazard events, tornadoes with a peak enhanced Fujita scale less than 5 are of the same size of earthquakes with a Richter magnitude

between 5 and 6. Even the tornado event with the largest size, the 2013 El Reno tornado, only has a magnitude equivalent to less than an earthquake Richter magnitude of 6 (see Fig. 4a). The lower bound of the enhanced Fujita scale for tornado approximates the threshold between tropical depression and tropical storm on the Saffir-Simpson hurricane wind scale (see Fig. 4). All recorded tornadoes are much smaller than hurricanes, as these tornadoes only have the sizes equivalent to the ones of tropical storms.

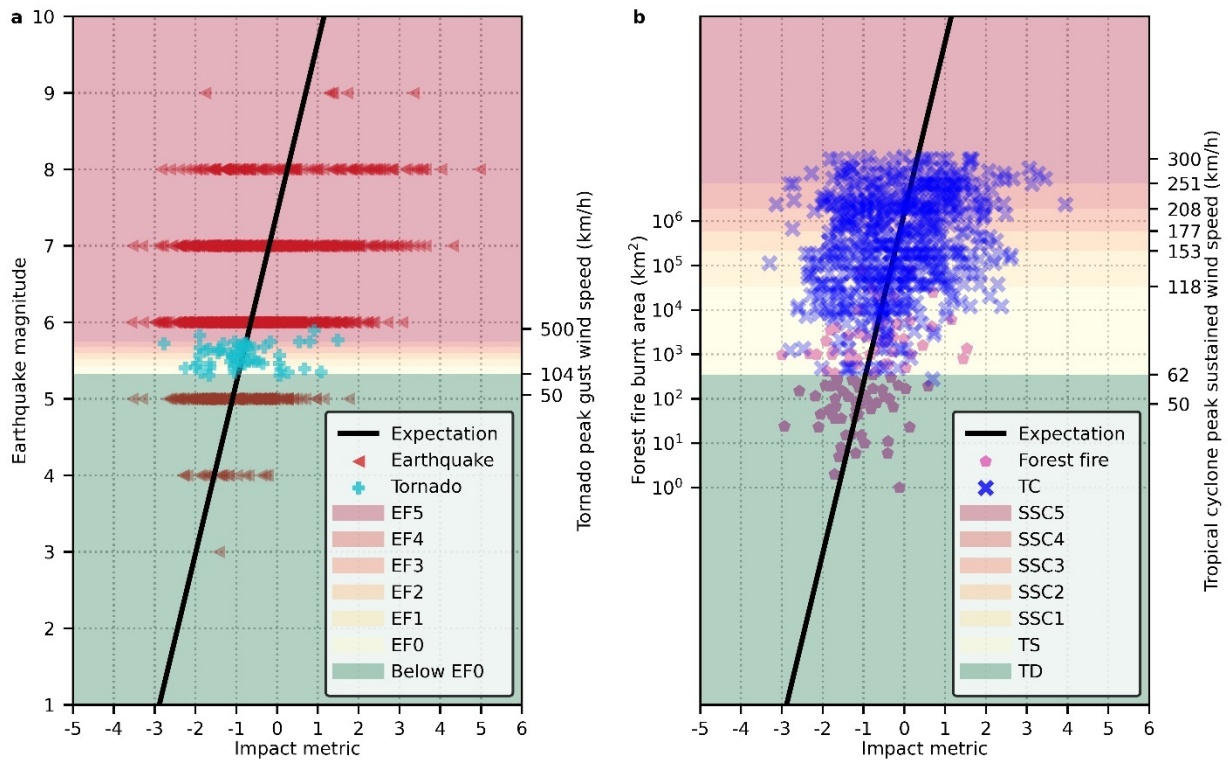

Fig. 4: Comparisons of magnitudes of earthquakes, tornadoes, forest fires, and tropical cyclones. a, Earthquake Richter magnitude versus tornado enhanced Fujita scale. EF0: enhanced Fujita scale 0 with gust wind speed at 104–137 km/h; EF1: enhanced Fujita scale 1 with gust wind speed at 138–177 km/h; EF2: enhanced Fujita scale 2 with gust wind speed at 178–217 km/h; EF3: enhanced Fujita scale 3 with gust wind speed at 218–266 km/h; EF4: enhanced Fujita scale 4 with gust wind speed at 267 – 322 km/h; EF5: enhanced Fujita scale 5 with gust wind speed over 322 km/h. **b**, Forest fire burnt area versus tropical cyclone Saffir-Simpson wind scale. TD: tropical depression with sustained wind speed at 62 km/h or below; TS: tropical storm with sustained wind speed at 63–118 km/h; SSC1: Saffir-Simpson category 1 with sustained wind speed at 119–153 km/h; SSC2: Saffir-Simpson category 2 with sustained wind speed at 154–177 km/h; SSC3: Saffir-Simpson category 3 with sustained wind speed at 178–208 km/h; SSC4: Saffir-Simpson category 4 with sustained wind speed at 209–251 km/h; SSC5: Saffir-Simpson category 5 with sustained

wind speed over 251 km/h; TC: tropical cyclone. Both **a** and **b** are plotted with the same range and scale with respect to the earthquake magnitude.

When comparing earthquakes with tropical cyclones, we notice that tropical cyclones tend to have sizes equivalent to earthquake magnitudes between 5 and 8 (see Fig. 4). A tropical cyclone with its peak Saffir-Simpson wind scale at category 2 is of the similar size as an earthquake with a magnitude of 7. Meanwhile, a magnitude 8 earthquake is equivalent in size to a tropical cyclone with its peak Saffir-Simpson wind scale at category 5. Within the data for this study, the tropical cyclone event with the largest equivalent magnitude (5.66) is Typhoon Meranti that affected the Philippines, Taiwan, mainland China, and South Korea in September 2016 and resulted in a total economic loss of around 70 million 2019 USD.

Compared to tropical cyclones, however, forest fires tend to have small equivalent magnitudes (see Fig. 4b). The two largest forest fires within the data were found to have an equivalent magnitude of 4.33 and occurred in Russia and Mongolia in 1996 resulting in 19 and 25 fatalities, respectively. Both forest fires are equivalent to a peak category 1 hurricane on the Saffir-Simpson wind scale in size. Many other recorded forest fire events only have an equivalent magnitude of a tropical depression.

Cold wave and heat wave events within the data have narrow ranges of equivalent magnitude of [4.54, 5.79] and [4.79, 5.67], respectively (see Supplementary Information Data 5). The range of minimum temperature of cold wave events from 0°C to –55°C is approximately equivalent to the range of maximum temperature of heat waves from 30°C to 55°C (see Fig. 5a). The strongest cold wave event recorded in the data, with its minimum temperature at –57°C, occurred in Russia in 2001 and killed 145 people, affected 6,120 more, and led to an economic loss of 100,000 2019 USD. The largest heat wave event, with its maximum temperature at 53°C, struck Pakistan in June 1991, resulting in 523 fatalities.

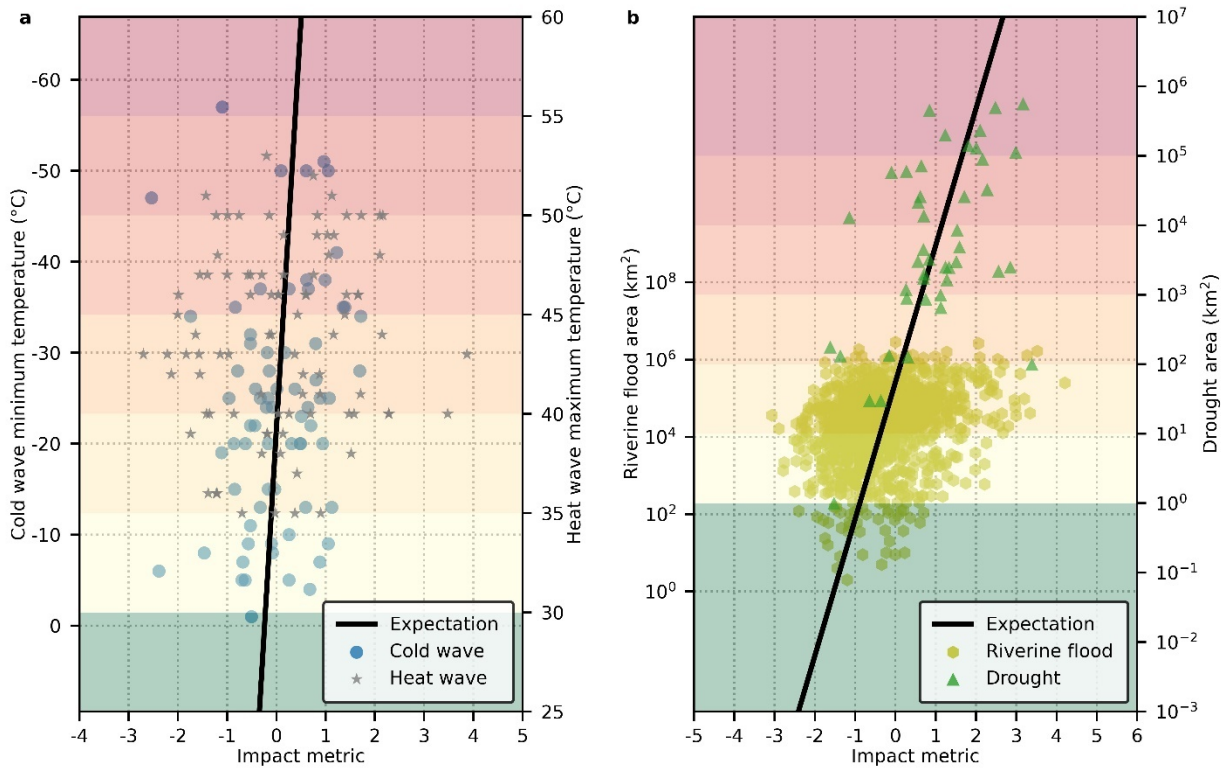

Fig. 5: Comparions of hazard magnitudes. a, Cold wave minimum temperature versus heat wave maximum temperature. **b**, Riverine flood area versus drought area.

The drought events included in this study have a large range of equivalent magnitude of [3.23, 9.07], while riverine floods have a small range of equivalent magnitude of [2.11, 5.59]. A riverine flood with a flooded area of hundreds of km^2 is equivalent in magnitude to a drought with an affected area of a few km^2 (see Fig. 5). Meanwhile, riverine floods with a flooded area of 1 million km^2 have the similar magnitude as droughts with an affected area of 100 km^2. Compared to riverine floods, drought disasters tend to be much larger in magnitude, even though some riverine floods may have resulted in higher impacts. For example, the flood disaster in mainland China in 1998, with its equivalent magnitude at 4.99, resulted in over 3,600 fatalities, more than 238 million affected population, and an economic loss of 30 billion 2019 USD.

Sensitivity analysis

In this study, the impact metric was constructed as the principal component with respect to three impact variables. The sum of squares of the weights of impact variables for the principal component equals 1. To examine the effects of change of weights of impact variables within the impact metric on equivalent magnitude, we conducted a sensitivity analysis by 1) keeping the sum of squares of all weights of impact variables equal to 1, 2) maintaining the equal ratio of squares of the weights of two impact variables, and 3) altering the weight of the third impact variable. As an example, Fig. 6 shows the result of a sensitivity analysis with data points of tsunami and flash flood. The data points are plotted based on their equivalent magnitudes with a fixed scale of the magnitude indicator of tsunami. When the weight of each of the impact variables of fatality (Figs. 6a-d), total affected population (Figs. 6e-h), and total economic damage (Figs. 6i-l) is shifted from 0 to 1, there are identifiable increasing or decreasing trends of alterations of the distributions of data points and the deviations between clusters of data points of the two different hazard types. However, when the weights of impact variables are far away from the extreme values of 0 and 1,

185 there is no significant change regarding the distribution of data points with respect to the equivalent

186 magnitude (see Figs. 6b, 6c, 6f, 6g, 6j, and 6k).

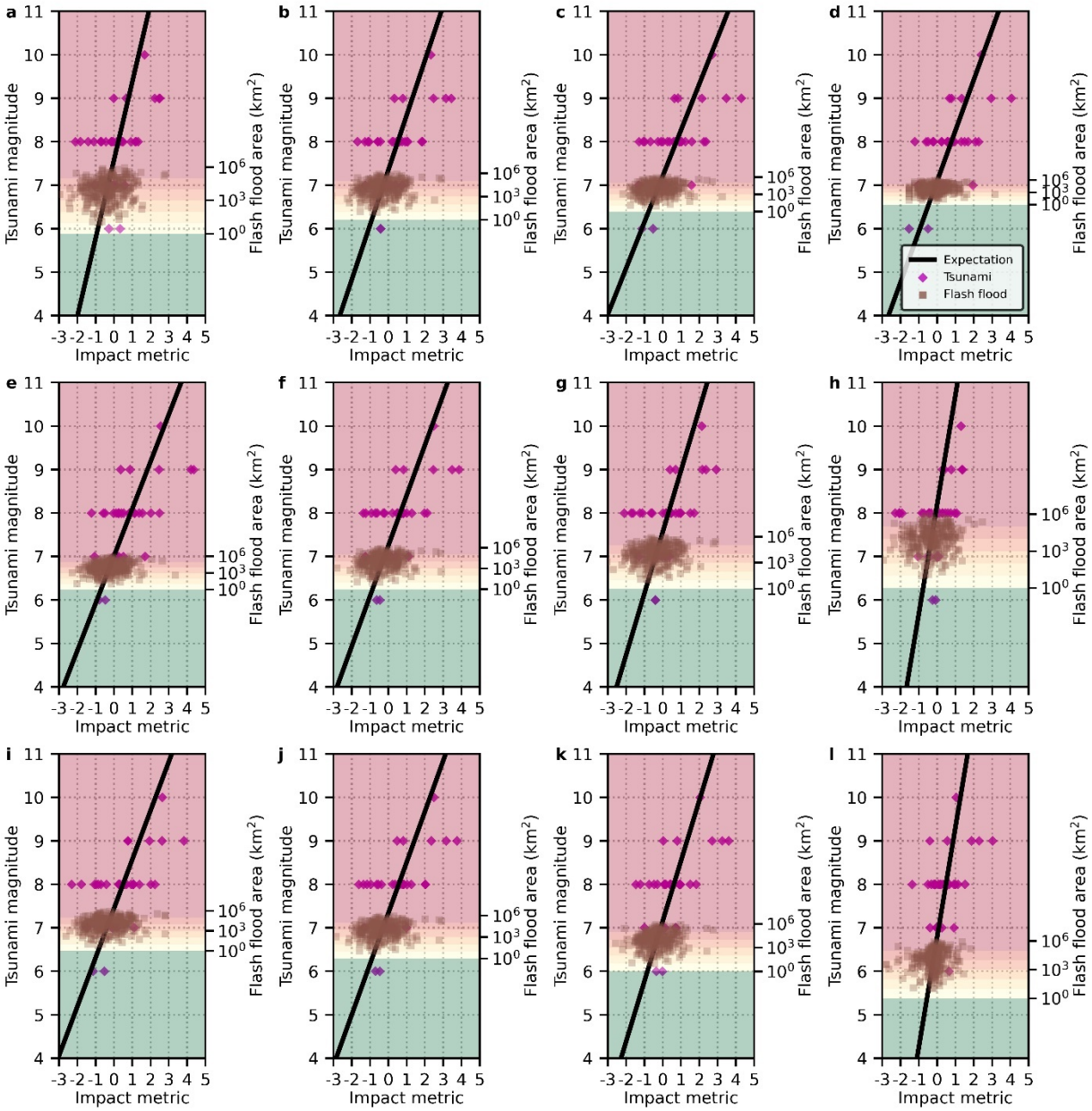

Fig. 6: Results of sensitivity analysis regarding effects of change of weight of one impact variable on equivalent magnitudes of tsunami and flash floods. a, Fatality weight equals 0. **b**, Fatality weight equals $\sqrt{w_{\mathrm{F}}^2/2}$, where w_{F} is the weight of fatality in the principal component. **c**, Fatality weight equals $\sqrt{(w_{\mathrm{F}}^2+1)/2}$. **d**, Fatality weight equals 1. **e**, Total affected population weight

equals 0. **f**, Total affected population weight equals $\sqrt{w_{\mathrm{TA}}^2/2}$, where w_{TA} is the weight of total affected population in the principal component. **g**, Total affected population weight equals $\sqrt{(w_{\mathrm{TA}}^2 + 1)/2}$. **h**, Total affected population weight equals 1. **i**, Total damage weight equals 0. **j**, Total damage weight equals $\sqrt{w_{\mathrm{TD}}^2/2}$, where w_{TD} is the weight of total damage in the principal component. **k**, Total damage weight equals $\sqrt{(w_{\mathrm{TD}}^2 + 1)/2}$. **l**, Total damage weight equals 1. In **a-l**, sum of squared weights of three impact variables equals 1 and the ratio of squares of the other two variable weights are kept constant.

Discussion

The development of Gardoni Scale for natural hazard events has several merits. First, professionals in natural hazard and disaster management may use the proposed equivalent magnitudes to facilitate hazard communication among various stakeholders. Similarly, journalists and the news media may also adopt the Gardoni Scale for their news reporting on natural disasters to the public. In addition, the computation of equivalent magnitudes may improve risk analysis within a multi-hazard context to augment decision making regarding resource allocation for mitigation, preparedness, response, and recovery against natural disasters. Following the proposal of the Gardoni Scale, we further suggest using the term *hazard equivalency* to refer to a new area of research in equivalent hazard scales, including both the agential and locational scales. To enhance local hazard management, future work needs to focus on exploration in locational equivalent hazard scales to indicate the severity of hazard events experienced by local communities.

Regarding the derivation of equivalent magnitudes in this study, the data points are in general centred along the expectation line (see Fig. 3). This implies that the derived equivalent magnitudes correspond well to the expectations of impact metric across all considered natural hazards. For some hazards, such as tornado, heat wave, cold wave, and flash flood, their ranges of equivalent magnitude among the available data points are small (see Supplementary Information Data 5). These small ranges of equivalent magnitude are associated with small absolute values of estimations of coefficients of magnitude indicators in the simple linear regression models (see Figs. 2a, 2f, 2h, and 2j, Table 4, and Supplementary Information Data 4). This suggests that hazard magnitudes of these natural hazard events may have some effects on hazard impacts. Meanwhile, factors of experiences of local communities, exposure, and social, structural, and environmental

vulnerability may play a bigger role in contributing to disastrous impacts of events of these natural hazards than the sheer magnitudes of the events.

In addition, given a certain value of equivalent magnitude, the variation of observed impact metrics can be large (see Fig. 3). Such a variation is likely to be caused by factors of exposure and vulnerability of local communities. If there are only a small proportion of all possible data points that can be collected for one natural hazard and the collected data points are limited to a specific region with a high exposure or vulnerability, the derived equivalent magnitude may be overestimated for that hazard. To reduce such a bias that can be potentially caused by exposure and vulnerability factors, we need to ideally collect data points of events for each natural hazard from a same wide geographical region and to consider events that have occurred during a same long period.

Future work may also need to improve the methodology for deriving the equivalent magnitudes by focusing on selections of magnitude indicators and impact variables. To demonstrate how to develop the equivalent magnitudes in this study, we only considered one magnitude indicator for each natural hazard. For some natural hazards, one magnitude indicator may not represent the true size of an event. For example, a tropical cyclone may result in disastrous impacts due to both wind and precipitation[30]. On the other hand, only three impact variables were taken into consideration in this study. Because natural hazard events may lead to a variety of other physical and social impacts[31–34], more impact variables need to be included in future work. Additionally, more efforts need to be made to derive the optimal impact metric based on the most pertinent impact variables for different natural hazards.

Methods

Data

No statistical methods were used to predetermine sample size. No randomized experiments were involved in the study. Data were gathered from the EM-DAT database[27]. We only included data points with values of magnitude indicators in this study (see Supplementary Information Data 7).

Derivation of impact metric

The impact metric was designed as the principal component of three logarithmically transformed and standardized impact variables. The selected three impact variables represent three major impact dimensions. The first impact variable, fatality, indicates the number of people killed in a natural hazard event. The second impact variable, total affected population, refers to the sum of numbers of residents injured, made homeless, or affected but not killed by the natural hazard event. The third impact variable, total damage, indicates the total amount of damage to property, crops, and livestock in 2019 USD caused by the natural hazard event[27]. The values of the impact variables were first logarithmically transformed to be within the range $(-\infty, \infty)$. The means and standard deviations of the logarithmically transformed impact variables were then applied to standardize the logarithmically transformed impact variables (see Table 1) with the formula

$$IV = \frac{\ln(IVO) - \mu_{\ln IV}}{\sigma_{\ln IV}} \tag{1}$$

where IV denotes the logarithmically transformed and standardized impact variable, IVO is the original impact variable, $\mu_{\ln IV}$ and $\sigma_{\ln IV}$ are respectively the mean and standard deviation of the logarithmically transformed impact variable. The principal component corresponds to the dimension, along which the variation of the data points is preserved to the largest extent in the 3-dimensional vector space. The principal component also shows the direction of the eigenvector

associated with the largest eigenvalue with respect to the covariance matrix of the three impact variables. Each data point represents the impact of one natural hazard event experienced by one country (see Fig. 1 and Supplementary Information Video 1).

To reduce the bias caused by factors of local exposure and vulnerability on hazard impact, we included all available data points at the country-year level for countries around the world and events from 1900 to 2020 to construct the impact metric for the twelve considered natural hazards. For derivation of the impact metric, we only kept data points (n = 1,470) without any missing values of the impact variables. A multiple linear regression was then conducted to determine the weights of impact variables. The resulting formula for impact metric is

$$IM = 0.6158IV_{\mathrm{F}} + 0.6215IV_{\mathrm{TA}} + 0.4843IV_{\mathrm{TD}} \tag{2}$$

where IM denotes the impact metric and IV_{F}, IV_{TA}, and IV_{TD} refer respectively to the impact variables of fatality, total affected population, and total damage.

Missing values and data aggregation

With the same data points for derivation of impact metric, we also calibrated six simple linear regression models and three bi-variate linear regression models. These regression models were created to fill in missing values of impact variables for data points with at most two empty entries among the three impact variables. Within each of these nine linear regression models, the dependent variable is one of the three impact variables. For each of the six simple linear regression models, the independent variable is one of the two impact variables that are not used as the dependent variable. The simple linear regression models have the form

$$IV_1 = a_1 + b_1 IV_2 + \sigma_1 \varepsilon \tag{3}$$

where $a_1 = 0$ and b_1 are two model coefficients, IV_1 and IV_2 are two considered impact variables, σ_1 is the dispersion parameter, and ε is a standard normal random variable. The statistics of

parameters of these simple linear regression models are shown in Table 2. Per the three bi-variate linear regression models, the independent variables are the two impact variables other than the one used as the dependent variable. The formula for the bi-variate linear regression models is

$$IV_1 = a_2 + b_2 IV_2 + c_2 IV_3 + \sigma_2 \varepsilon \quad (4)$$

where $a_2 = 0$, b_2, and c_2 are three model coefficients, IV_3 is the third impact variable, and σ_2 is the dispersion parameter. Table 3 lists the statistics of parameters of the bi-variate linear regression models. By applying the derived linear regression models, we filled in the missing values of data points. We then aggregated data points event-wise and reached a total of 3,844 data points, each representing one unique hazard event.

Regression models for individual hazards

Before conducting regressions for deriving the equivalent magnitudes, we removed the data points with questionable values of magnitude indicators. For cold wave events, we only considered data points with a minimum temperature ≤0°C; for convective storms, we only included data points with a peak gust wind speed ≥60 km/h; for forest fires, we only considered data points with a burnt area ≤200,000 km^2; for heat wave events, we only included data points with a maximum temperature ≥35°C and ≤57°C; for tornadoes, we only considered data points with a peak gust wind speed ≥100 km/h; and for tsunami, we only included data points with an earthquake magnitude ≥6. Magnitude indicators of most of the considered natural hazards were also logarithmically transformed to fit within the range (–∞, ∞). The magnitude indicators that were not logarithmically transformed include minimum temperature of cold wave, Richter magnitude of earthquake, maximum temperature of heat wave, and earthquake magnitude of tsunami. The minimum and maximum temperatures of cold wave and heat wave events were excluded from logarithmic transformations because temperature has a range [–273.15, ∞) and the lower bound of

temperature range, –273.15°C, is far away from 0. Meanwhile, there is no need to logarithmically transform earthquake magnitudes, as the range of earthquake magnitude is already (–∞, ∞).

To establish the relationship between the magnitude indicator and impact metric, we calibrated one simple linear regression model for each of the twelve considered natural hazards. In general, such a regression model can be written as

$$IM = a_3 + b_3 MI + \sigma_3 \varepsilon \tag{5}$$

where a_3 and b_3 are two model coefficients, MI denotes the magnitude indicator, and σ_3 is the dispersion parameter. The statistics of parameters of these twelve regression models are listed in Table 4. Parameters of all linear regression models involved in this study were determined with the maximum likelihood approach with a Raphson's algorithm[34–37]. For each regression model, the standard errors of the parameter estimates are derived from the main diagonal of the covariance matrix of model parameters computed as the negative inverse of the observed Fisher information matrix.

Equivalent magnitude formula

To present the equivalent magnitude roughly within the range from 0 to 10, we applied a linear transformation to the point estimate of impact metric

$$EM = \widehat{E}(IM) \times 2 + 5 \tag{6}$$

where EM refers to the equivalent magnitude and $\widehat{E}(\cdot)$ denotes the point estimate of expectation. The derived equivalent magnitudes of the 3,844 natural hazard events are recorded in Supplementary Information Data 6.

Data availability

The data that support the findings of this study are available within the Supplementary Information Data 7 file.

Code availability

Python codes used to generate the results of this study are included within the Supplementary Information Codes file.

References

1. Richter, C. F. An instrumental earthquake magnitude scale. *B. Seismol. Soc. Am.* **25**, 1–32 (1935).
2. National Hurricane Center & Central Pacific Hurricane Center. *Saffir-Simpson Hurricane Wind Scale* (2020); https://www.nhc.noaa.gov/aboutsshws.php
3. Fujita, T. T. *Proposed Characterization of Tornadoes and Hurricanes by Area and Intensity* (1971); https://ntrs.nasa.gov/search.jsp?R=19720008829
4. Potter, S. Fine-tuning Fujita: After 35 years, a new scale for rating tornadoes takes effect. *Weatherwise* **62**, 64–71 (2007).
5. Wood, H. O. & Neumann, F. Modified Mercalli intensity sale of 1931. *B. Seismol. Soc. Am.* **21**, 277–283 (1931).
6. Wald, D. J., Worden B. C., Quitoriano, V. & Pankow, K. L. *ShakeMap Manual: Technical Manual, Users Guide, and Software Guide* (2006); https://doi.org/10.3133/tm12A1
7. Lekkas, E. L., Andreadakis, E., Kostaki, I. & Kapourani, E. A proposal for a new Integrated Tsunami Intensity Scale (IT IS-2012). *B. Seismol. Soc. Am.* **103**, 1493–1502 (2013).

8. Steadman, R. G. The assessment of sultriness. Part I: A temperature-humidity index based on human physiology and clothing science. *J. Appl. Meteorol.* **18**, 861–873 (1979).

9. National Weather Service. *Heat Index* (2019); https://www.weather.gov/safety/heat-index

10. Papathoma-Köhle, M., Cristofari, G., Wenk, M. & Fuchs, S. The importance of indicator weights for vulnerability indices and implications for decision making in disaster management. *Int. J. Disast. Risk Re.* **36**, 101103 (2019).

11. Merz, B. et al. Impact forecasting to support emergency management of natural hazards. *Rev. Geophys.* **58**, e2020RG000704 (2020).

12. Shcherbakov, R., Zhuang, J., Zöller, G. & Ogata, Y. Forecasting the magnitude of the largest expected earthquake. *Nat. Commun.* **10**, 4051 (2019).

13. Kanamori, H. The energy release in great earthquakes. *J. Geophys. Res.* **82**, 2981–2987 (1977).

14. Abe, K. Size of great earthquakes of 1837–1974 inferred from tsunami data. *J. Geophys Res.* **84**, 1561–1568 (1979).

15. Murty, T. S. & Loomis, H. G. A new objective tsunami magnitude scale. *Mar. Geod.* **4**, 267–282 (1980).

16. Arbanas, S. M. & Arbanas, Ž. Landslides: A guide to researching landslide phenomena and processes. In N. Gaurina-Medjimurec (Ed.) *Handbook of Research on Advancements in Environmental Engineering*, Hershey, PA: IGI Global, 474–510 (2015).

17. Tanyaş, H., Allstadt, K. E. & van Westen, C. J. An updated method for estimating landslide-event magnitude. *Earth Surf. Proc. Land.* **43**, 1836–1847 (2018).

18. Walker, G. P. L. Explosive volcanic eruptions – A new classification scheme. *Geol. Rundsch.* **62**, 431–446 (1973).

19. Newhall, C. G. & Self, S. The volcanic explosivity index (VEI): An estimate of explosive magnitude for historical volcanism. *J. Geophys. Res.* **87**, 1231–1238 (1982).

20. Bell, G. D. et al. Climate assessment for 1999. *B. Am. Meteorol. Soc.* **81**, S1–S50 (1999).

21. Emanuel, K. Increasing destructiveness of tropical cyclones over the past 30 years. *Nature* **436**, 686–688 (2005).

22. Kossin, J. P., Knapp, K. R., Olander, T. L. & Velden, C. S. Global increase in major tropical cyclone exceedance probability over the past four decades. *P. Natl. Acad. Sci. USA* **117**, 11975–11980 (2020).

23. Palmer, W. C. *Meteorological Drought* (1965); https://www.ncdc.noaa.gov/temp-and-precip/drought/docs/palmer.pdf

24. Singh, G. R., Jain, M. K. & Gupta, V. Spatiotemporal assessment of drought hazard, vulnerability and risk in the Krishna River basin, India. *Nat. Hazards* **99**, 611–635 (2019).

25. Gardoni, P. & Murphy, C. Capabilities-based approach to measuring the societal impacts of natural and man-made hazards in risk analysis. *Nat. Hazards Rev.* **10**, 29–37 (2009).

26. Gardoni, P. & Murphy, C. A scale of risk. *Risk Anal.* **34**, 1208–1227 (2014).

27. Guha-Sapir, D., Hoyois, P. & Below, R. *EM-DAT Public* (2020); https://public.emdat.be/

28. Jolliffe, I. T. *Principal Component Analysis, Second Edition*, New York, NY: Springer (2002).

29. Jolliffe, I. T. & Cadima, J. Principal component analysis: A review and recent developments. *Phil. Trans. R. Soc. A* **374**, 20150202 (2016).

30. Mudd, L., Rosowsky, D., Letchford, C. & Lombardo, F. Joint probabilistic wind–rainfall model for tropical cyclone hazard characterization. *J. Struct. Eng.* **143**, 04016195 (2017).

31. Lindell, M. K. & Prater, C. S. Assessing community impacts of natural disasters. *Nat. Hazards Rev.* **4**, 176–185 (2003).

32. Gardoni, P. & Murphy, C. Gauging the societal impacts of natural disasters using a capability approach. *Disasters* **34**, 619–636 (2010).

33. Wang, Y. (V.) et al. *Assessing Socioeconomic Impacts of Cascading Infrastructure Disruptions Using the Capability Approach* (2016); https://apps.dtic.mil/sti/citations/AD1016582

34. Wang, Y. (V.), Gardoni, P., Murphy, C. & Guerrier, S. Empirical predictive modeling approach to quantifying social vulnerability to natural hazards. *Ann. Am. Assoc. Geogr.* (in press).

35. Wang, Y. (V.), Gardoni, P., Murphy, C. & Guerrier, S. Predicting fatality rates due to earthquakes accounting for community vulnerability. *Earthq. Spectra* **35**, 513–536 (2019).

36. Wang, Y. (V.) & Sebastian, A. G. Community flood vulnerability and risk assessment: An empirical predictive modelling approach. *J. Flood Risk Manag.* (under review).

37. Wang, Y. (V.) Empirical local Hazard models for bolide explosions. *Nat. Hazards Rev.* **21**, 04020037 (2020).

Acknowledgements

We thank Professor Paolo Gardoni and Professor Colleen Murphy for discussions and suggestions.

Author contributions

Y.(V.)W. was responsible for design of the study, data collection, data processing, and coding. Data analysis and drafting and critical review of the manuscript was undertaken by both authors.

Competing interests

The authors declare no competing interests.

Correspondence and requests for materials

Correspondence and requests for materials should be addressed to Y.(V.)W.

Table 1: Means and standard deviations of original and logarithmically transformed impact variables used in the study[a]

Variable	Unit	Original mean	Original standard deviation	Logarithmically transformed mean	Logarithmically transformed standard deviation
Fatality	People	1.31×10^{3}	1.18×10^{4}	3.3892	2.1999
Total affected population	People	1.38×10^{6}	9.47×10^{6}	10.4116	3.1618
Total damage	1,000 2019 USD	1.36×10^{6}	8.45×10^{6}	11.1889	2.6304

[a]This table corresponds to Supplementary Information Data 1.

425 **Table 2: Statistics of parameters of six simple linear regression models for filling in missing**

426 **values of impact variables**[a]

Model number	**Dependent variable**	**Independent variable**	b_1	σ_1
I1	Fatality	Total affected	0.5096 (0.0224)	0.8604 (0.0159)
I2	Fatality	Total damage	0.2802 (0.0250)	0.9599 (0.0177)
I3[b]	Total affected	Fatality	0.5096 (0.0224)	0.8604 (0.0159)
I4	Total affected	Total damage	0.2948 (0.0249)	0.9556 (0.0176)
I5[c]	Total damage	Fatality	0.2802 (0.0250)	0.9599 (0.0177)
I6[d]	Total damage	Total affected	0.2948 (0.0249)	0.9556 (0.0176)

427 [a]This table corresponds to Supplementary Information Data 2; R^2s are included in Fig. 1; standard

428 errors are in the parentheses; estimations of b_1 and σ_1 are all significant at $p < 10^{-20}$.

[b]Models I1 and I3 share the same model parameters and R^2.

[c]Models I2 and I5 share the same model parameters and R^2.

[d]Models I4 and I6 share the same model parameters and R^2.

Table 3: Statistics of parameters of three bi-variate linear regression models for filling in missing values of impact variables[a]

Model number	**Dependent variable**	**Independent variable 1**	**Independent variable 2**	b_2	c_2	σ_2
I7	Fatality	Total affected	Total damage	0.4676 (0.0232)	0.1423 (0.0232)	0.8496 (0.0157)
I8	Total affected	Fatality	Total damage	0.4633 (0.0230)	0.1650 (0.0230)	0.8457 (0.0156)
I9	Total damage	Fatality	Total affected	0.1755 (0.0286)	0.2054 (0.0286)	0.9435 (0.0174)

[a]This table corresponds to Supplementary Information Data 3; R^2s are included in Fig. 1; standard errors are in the parentheses; estimations of b_2, c_2, and σ_2 are all significant at $p < 10^{-8}$.

Table 4: Statistics of parameters of twelve simple linear regression models for deriving equivalent magnitudes[a]

Model number	Hazard	a_3	b_3	σ_3
M1	Cold wave	–0.2404	–0.0111	0.8595
		(0.2171)	(0.0080)	(0.0726)***
M2	Convective storm	–7.5637	1.3755	0.7812
		(2.1192)*	(0.4309)*	(0.0977)***
M3	Drought	–0.8833	0.2206	1.0162
		(0.4691)	(0.0524)**	(0.1083)***
M4	Earthquake	–3.3328	0.4484	1.2464
		(0.2308)***	(0.0361)***	(0.0246)***
M5	Extra-tropical storm	–12.2505	2.2827	1.3672
		(6.6008)	(1.2965)	(0.1973)***
M6	Flash flood	–1.0275	0.0701	0.9417
		(0.2244)***	(0.0238)*	(0.0392)***
M7	Forest fire	–1.6116	0.1131	0.8147
		(0.2221)***	(0.0355)*	

				(0.0568)***
M8	Heat wave	–0.9524	0.0243	1.3297
		(1.3678)	(0.0310)	(0.1002)***
M9	Riverine flood	–1.5284	0.1226	1.0140
		(0.1349)***	(0.0133)***	(0.0209)***
M10	Tornado	–1.7272	0.1683	0.8511
		(1.5488)	(0.2920)	(0.0784)***
M11	Tropical cyclone	–4.2569	0.8016	1.1719
		(0.6510)***	(0.1273)***	(0.0326)***
M12	Tsunami	–7.0781	0.9681	1.2054
		(2.0108)*	(0.2528)**	(0.1484)***

441 [a]This table corresponds to Supplementary Information Data 4; R^2s are included in Fig. 2; standard
442 errors are in the parentheses.
443 *$p < 10^{-2}$; **$p < 10^{-3}$; ***$p < 10^{-5}$.

444

Figures

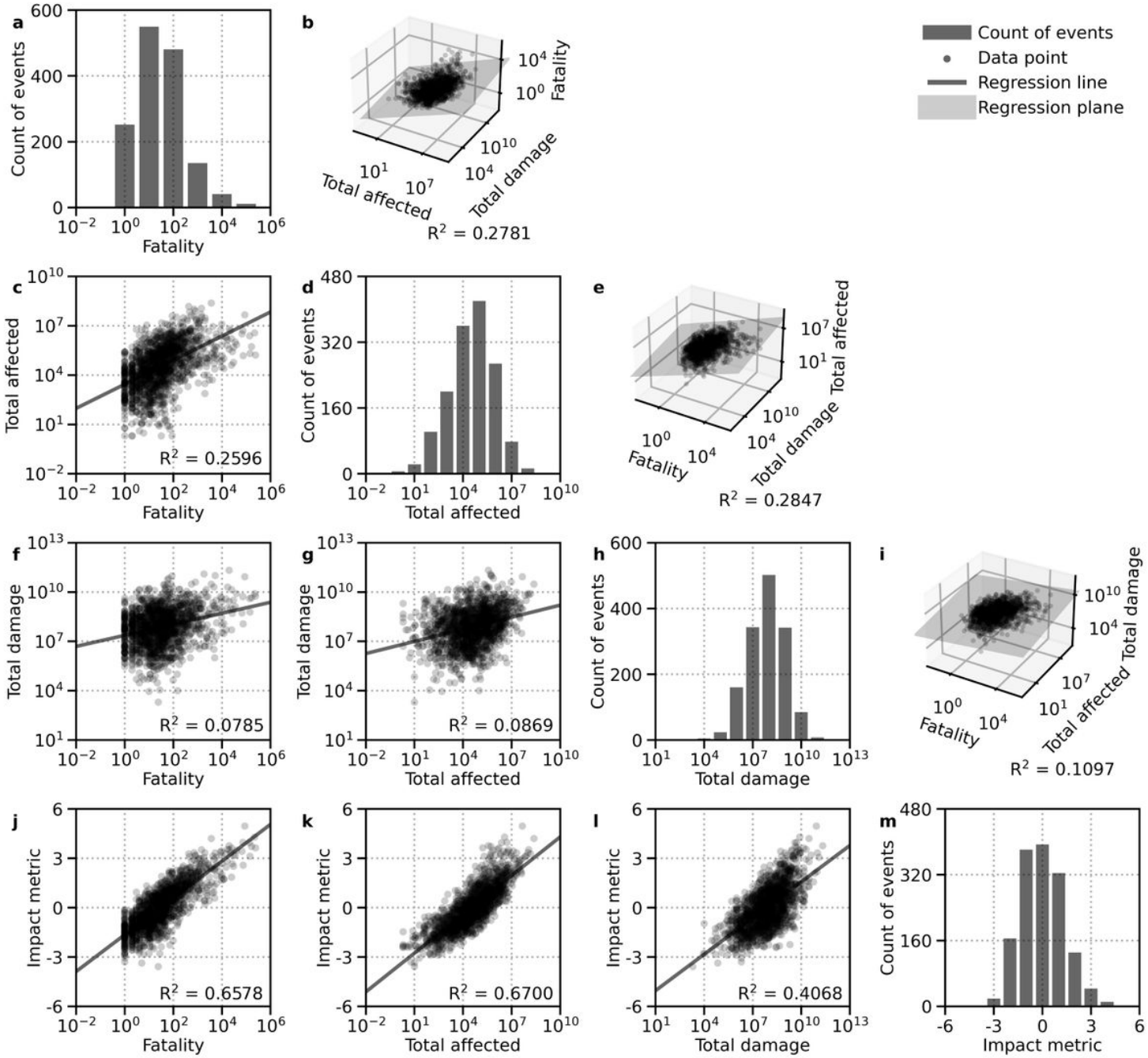

Figure 1

Impact variables and impact metric. a, Histogram of impact variable fatality. b, Fatality regressed on total affected population and total damage in 2019 USD with a multiple linear regression. c, Total affected population regressed on fatality with a simple linear regression. d, Histogram of impact variable total affected population. e, Total affected population regressed on fatality and total damage in 2019 USD with a multiple linear regression. f, Total damage in 2019 USD regressed on fatality with a simple linear regression. g, Total damage in 2019 USD regressed on total affected population with a simple linear

regression. h, Histogram of impact variable total damage in 2019 USD. i, Total damage in 2019 USD regressed on fatality and total affected population with a multiple linear regression. j, Impact metric regressed on fatality with a simple linear regression. k, Impact metric regressed on total affected population with a simple linear regression. l, Impact metric regressed on total damage in 2019 USD with a simple linear regression. m, Histogram of impact metric.

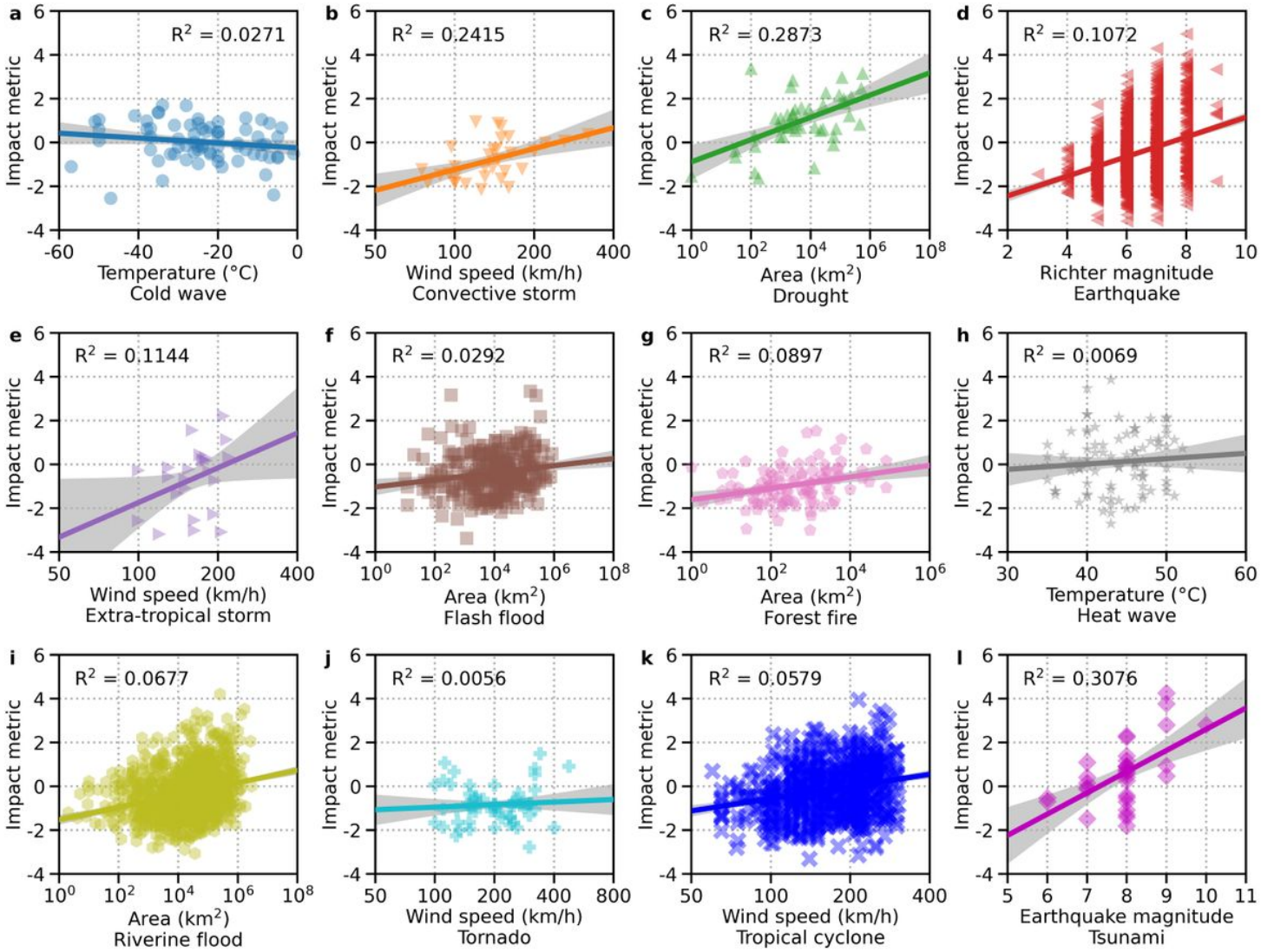

Figure 2

Simple linear regressions on impact metric against magnitude indicators. a, Impact metric regressed on minimum temperature of cold wave. b, Impact metric regressed on peak gust wind speed of convective storm. c, Impact metric regressed on total area of drought. d, Impact metric regressed on Richter magnitude of earthquake. e, Impact metric regressed on peak gust wind speed of extra-tropical storm. f, Impact metric regressed on total flooded area of flash flood. g, Impact metric regressed on total burnt area of forest fire. h, Impact metric regressed on maximum temperature of heat wave. i, Impact metric regressed on total flooded area of riverine flood. j, Impact metric regressed on peak gust wind speed of tornado. k, Impact metric regressed on maximum sustained wind speed of tropical cyclone. l, Impact

metric regressed on earthquake magnitude of tsunami. Solid lines are regression lines. Shaded areas are the 95% confidence intervals of the corresponding regression lines.

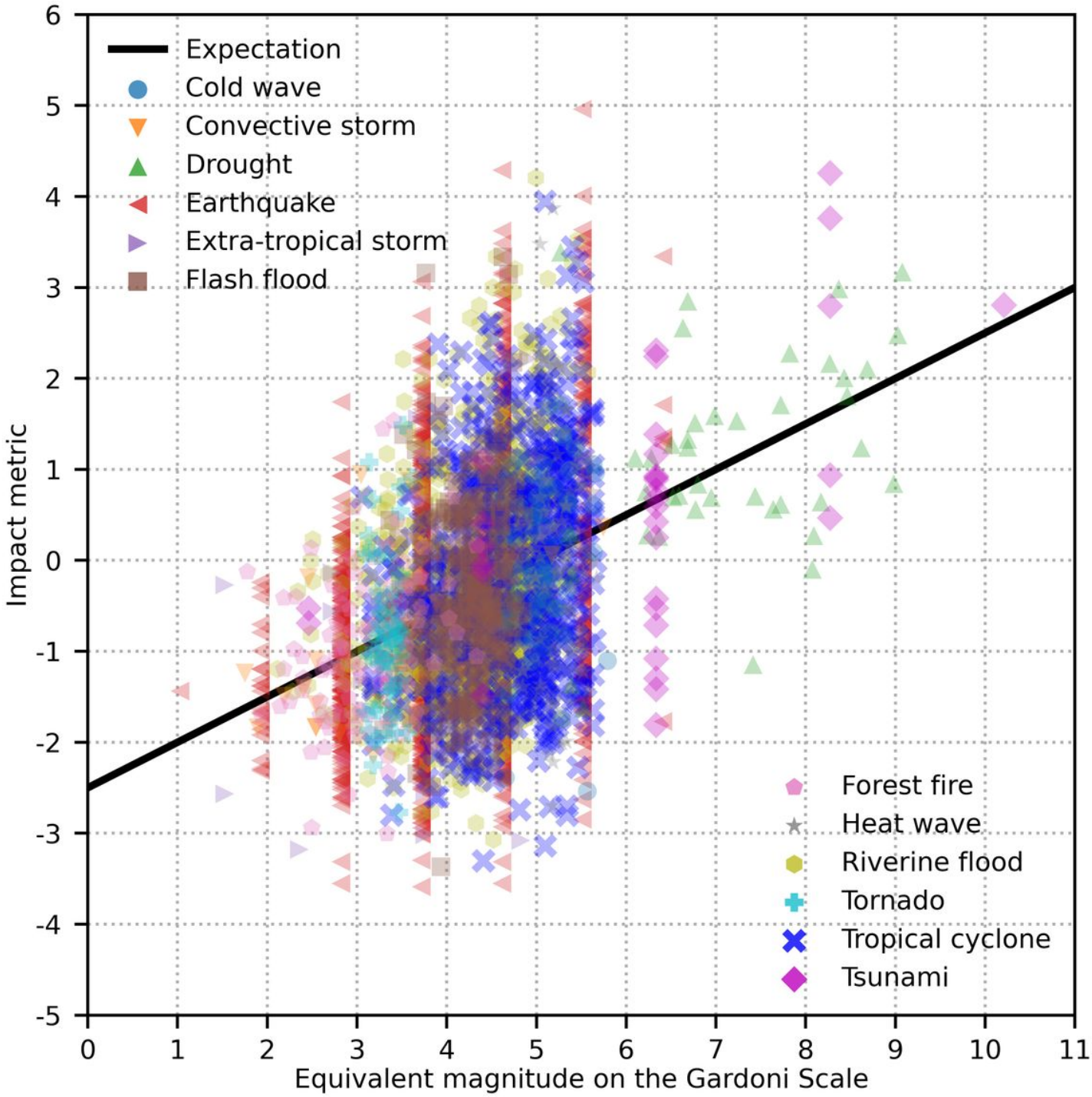

Figure 3

Impact metric versus equivalent magnitude. The expectation line shows the values of the expected impact metric with respect to equivalent magnitude on the Gardoni Scale.

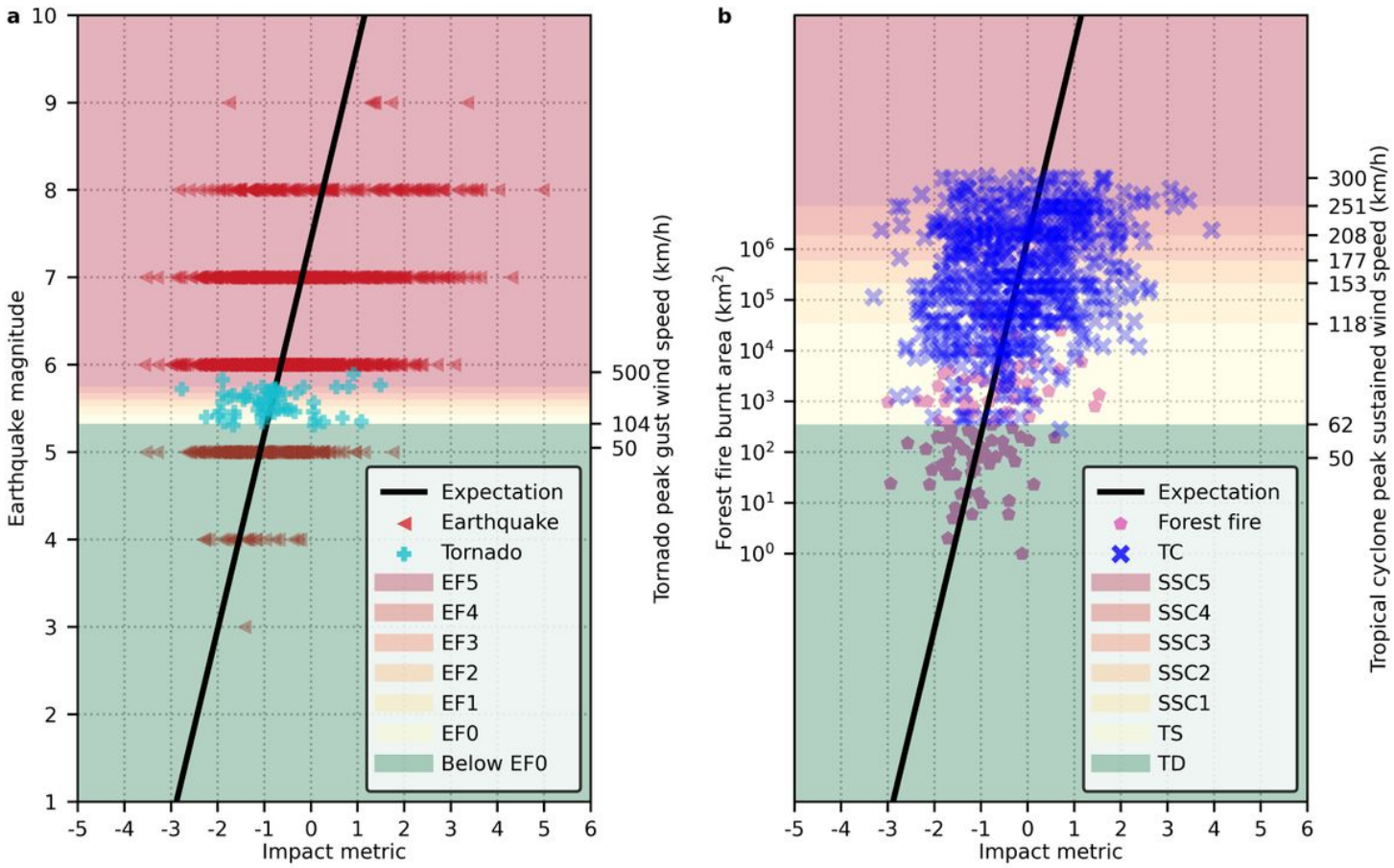

Figure 4

Comparisons of magnitudes of earthquakes, tornadoes, forest fires, and tropical cyclones. a, Earthquake Richter magnitude versus tornado enhanced Fujita scale. EF0: enhanced Fujita scale 0 with gust wind speed at 104–137 km/h; EF1: enhanced Fujita scale 1 with gust wind speed at 138–177 km/h; EF2: enhanced Fujita scale 2 with gust wind speed at 178–217 km/h; EF3: enhanced Fujita scale 3 with gust wind speed at 218–266 km/h; EF4: enhanced Fujita scale 4 with gust wind speed at 267 – 322 km/h; EF5: enhanced Fujita scale 5 with gust wind speed over 322 km/h. b, Forest fire burnt area versus tropical cyclone Saffir-Simpson wind scale. TD: tropical depression with sustained wind speed at 62 km/h or below; TS: tropical storm with sustained wind speed at 63–118 km/h; SSC1: Saffir-Simpson category 1 with sustained wind speed at 119–153 km/h; SSC2: Saffir-Simpson category 2 with sustained wind speed at 154–177 km/h; SSC3: Saffir-Simpson category 3 with sustained wind speed at 178–208 km/h; SSC4: Saffir-Simpson category 4 with sustained wind speed at 209–251 km/h; SSC5: Saffir-Simpson category 5 with sustained wind speed over 251 km/h; TC: tropical cyclone. Both a and b are plotted with the same range and scale with respect to the earthquake magnitude.

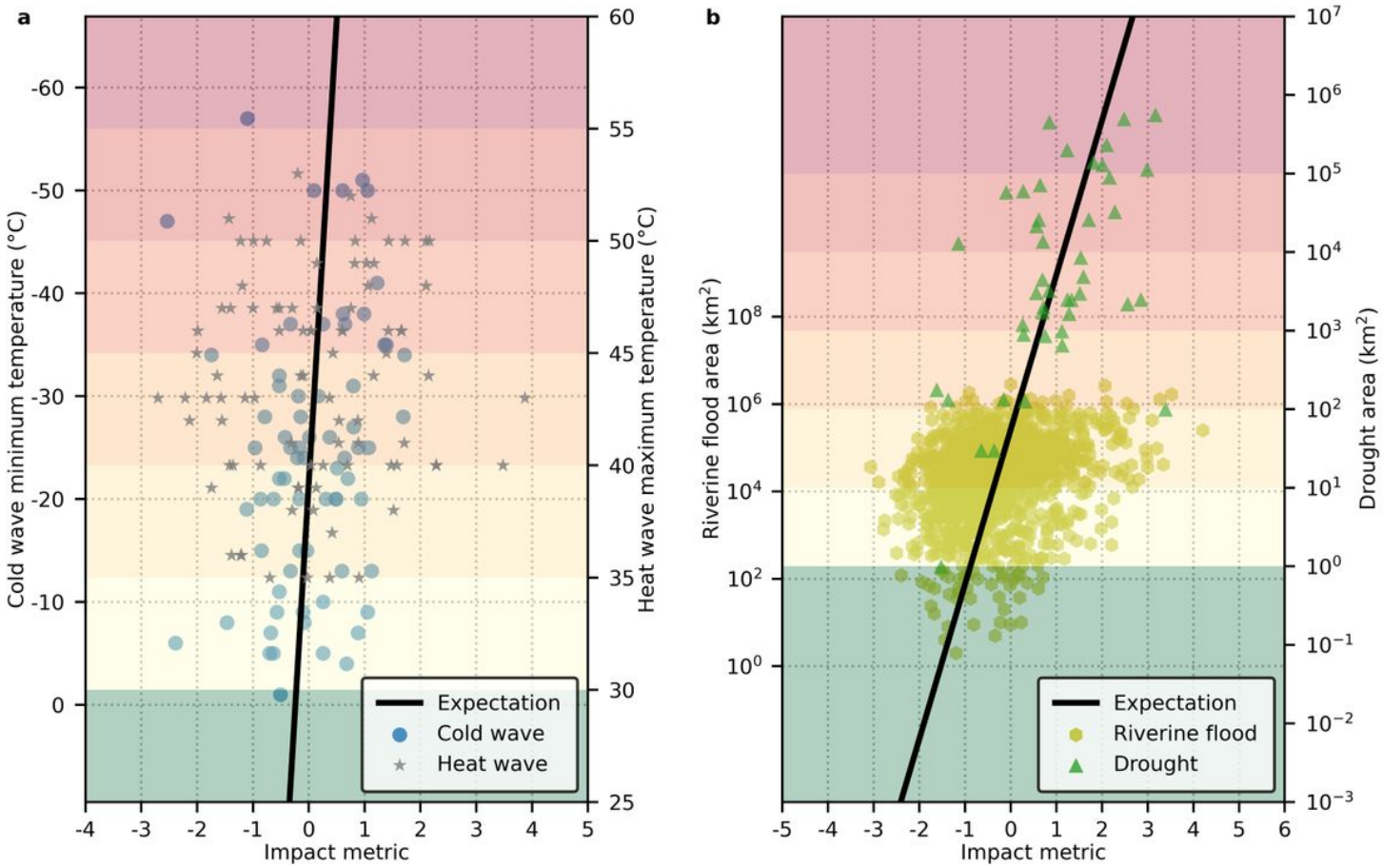

Figure 5

Comparions of hazard magnitudes. a, Cold wave minimum temperature versus heat wave maximum temperature. b, Riverine flood area versus drought area.

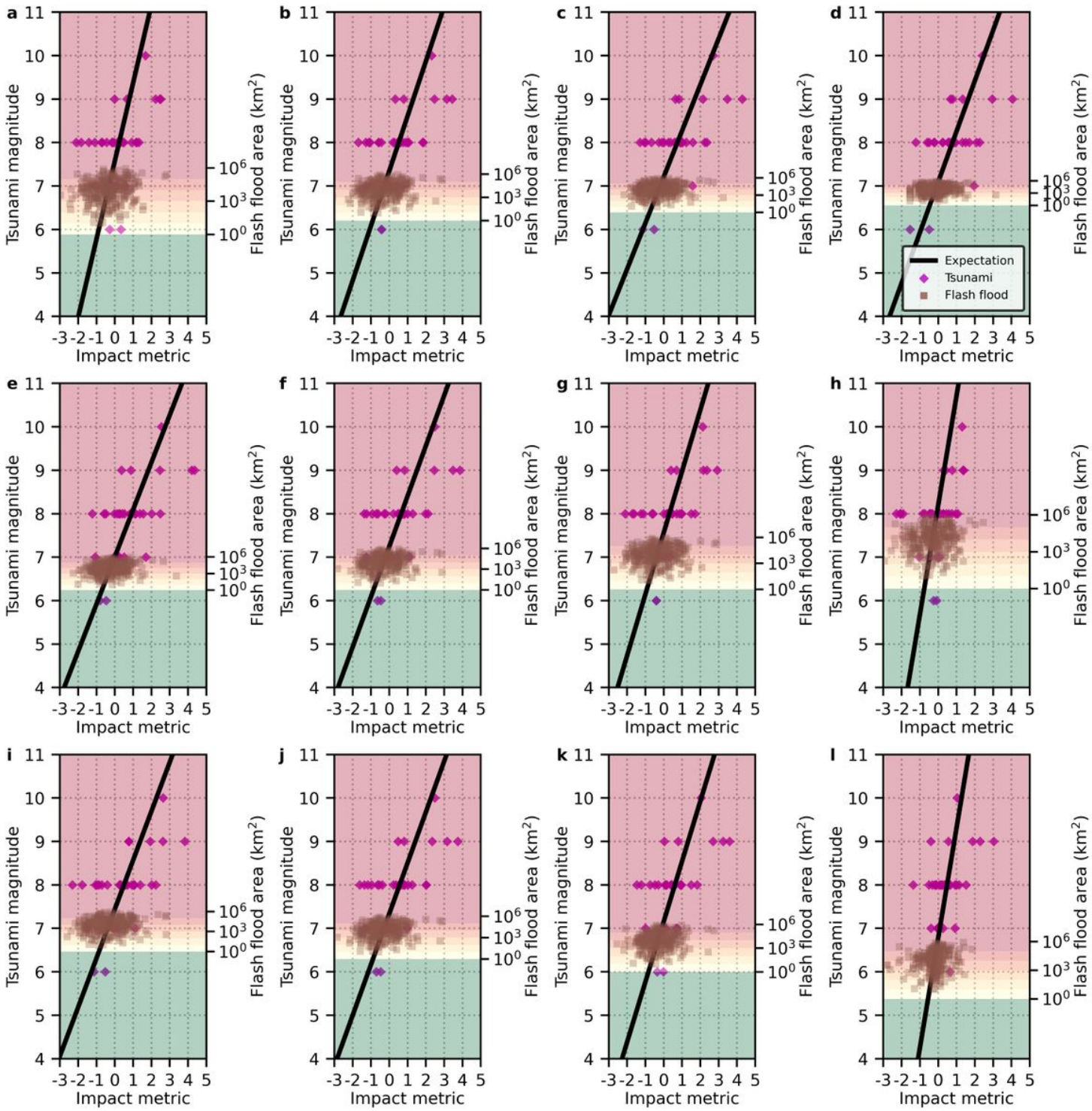

Figure 6

see .pdf for caption

Supplementary Files

This is a list of supplementary files associated with this preprint. Click to download.

- SupplementaryInformationVideo1.mp4
- SupplementaryInformationCodes.txt
- SupplementaryInformationData1.pdf
- SupplementaryInformationData2.pdf
- SupplementaryInformationData3.pdf
- SupplementaryInformationData4.pdf
- SupplementaryInformationData5.pdf
- SupplementaryInformationData6.pdf
- SupplementaryInformationData7.zip